Bulletin of Engineering Geology and the Environment (2020) 79:3049–3062
https://doi.org/10.1007/s10064-020-01751-9

ORIGINAL PAPER

Study on engineering properties of sand strengthened by mixed fibers and polyurethane organic polymer

Jin Liu[1] · Fan Bu[1] · Yuxia Bai[1] · Zhihao Chen[1] · Debi Prasanna Kanungo[2] · Zezhuo Song[1] · Ying Wang[1] · Changqing Qi[1] · Jing Chen[1]

Received: 30 September 2019 / Accepted: 17 February 2020 / Published online: 24 February 2020

Abstract

A considerable number of engineering hazards are caused by loose internal structure of sands. Thus, many researchers have explored a variety of reinforcement methods. A new reinforcement technique was experimentally evaluated in this study. In particular, a hybrid method with a combination of fiber and polymer was studied. Three different types of fibers (sisal, polypropylene, and palm) in combination with varying concentrations of polymers were experimented to improve the internal structure and strength of sand samples reconstituted at different densities. Through a series of laboratory tests, the compressive and tensile strength variations of different combinations were obtained, and the interaction between fibers and polymer inside the sand was evaluated by scanning electron microscopy (SEM). The experimental results show that the tensile and compressive strength of the reinforced sand increases with the increase of the polymer concentration, sample density, and different fiber combinations. This provides some references for future practical engineering applications.

Keywords Polymer treatment · Fiber reinforcement · Hybrid soil composites · Strength properties

Introduction

Sand has a series of disadvantages such as lack of cohesion and loose structure between particles and high porosity. If not reinforced, these limitations in sand will cause a variety of engineering hazards (Helming et al., 2006; Wan and Fell, 2004; Xiao and Shwiyhat, 2012). For example, the stability of sandy slope was seriously compromised due to liquefaction caused by ground vibrations and erosion by seepage after intensive rainfalls. River bank sandy slopes suffer erosion and subsequent collapse resulting into channel blockage due to landslides and other disasters. Therefore, improving the stability of sand is a crucial task. Some researchers have used traditional methods to reinforce sand such as by adding cement, fly ash, and their mixtures (Chen and Wang, 2006; Kaniraj and Havanagi, 1999; Kawamura and Kasai, 2006; Kumar and Raju, 2009; Wang et al., 2018). Undoubtedly, the above research proves that adding cement and fly ash can effectively improve the overall structure and strength of sand. However, some deficiencies also emerged out by using these materials for sand stabilization. These deficiencies may be lack of vegetation growth on cement and fly ash-based reinforced sand, and increase in dust and CO_2 emissions polluting the environment in the process of cement production (Najim et al., 2014; Caravaca et al., 2017; El-Attar et al., 2017).

In recent years, many scientists have focused on exploring the non-traditional reinforcement techniques such as polymer reinforcement that has great potential in soil improvement with less eco-environmental impacts. Mohsin and Attia (2015) discussed the stability of the reinforced sand under different temperature conditions after adding different concentrations of polyacrylamide (PAM) solution. Zang et al. (2019) studied the effects of different segments in polyurethane structure on the performance of sand stabilization. Anamica and Pande (2018) presented a review on the synthesis, properties, and applications of polyacrylamide. The above studies have provided useful knowledge for the application of organic polymers in soil strengthening and explained the existence of polymer matrix greatly promoting the soil inter-particle connections. Apart from improving the internal structure and

✉ Jin Liu
jinliu920@163.com

[1] School of Earth Science and, Hohai University Nanjing, Nanjng 210098, Jiangsu, China

[2] CSIR-Central Building Research Institute (CBRI), Roorkee 247667, India

strength characteristics of sand, biopolymer treatment also enhances vegetation germination and soil water retention characteristics against evaporation, which can provide some effective method to control desertification (Chang et al., 2015; Liu et al., 2019).

In addition, many researchers have used different common fibers to reinforce sand because of their unique mechanical properties. Ye et al. (2017) conducted a series of undrained cyclic triaxial compression tests and hollow cylindrical torsional shear tests on saturated sand samples with and without fibers and found that the fiber-reinforced sand has improved resistance to liquefaction. Li et al. (2018) researched the tensile properties of fiber-reinforced sand under freeze-thaw conditions and found that the sand-fiber composite displays increased stiffness, peak strength, and residual strength, and also exhibits a change in failure behavior from brittle to more ductile in nature after first freeze-thaw cycle. Tang et al. (2016) observed that the soil tensile behavior can be improved by randomly distributed polypropylene fibers. Rekha et al. (2016) discussed the engineering performance of the sand reinforced with human hair fiber and the possibility of its application in pavement engineering. These studies on fiber-reinforced sand have highlighted its bright application prospects and, hence, worthy of further research.

Taking lead from the above research studies, the new method of fiber polymer composite-reinforced sand has attracted widespread attention from many researchers (Reis and Carneiro, 2012; Liu et al., 2017; Mirzababaei et al., 2018; Liu et al., 2018). However, study on mixed fiber polymer reinforcement as compared with single fiber polymer reinforcement is very rare. Hence, in this present work, an attempt will be made to reinforce sand with mixed fiber polymer, aiming to understand the reinforcement effect of mixed fibers and polyurethane organic polymer. During the whole research process, the direct tensile and the unconfined compressive tests are performed on reinforced sand samples with different fiber combinations, polymer concentrations, and densities. The reinforcement mechanism was analyzed by scanning electron microscopy (SEM). The present study is focused on evaluating the mixed fiber polymer reinforcement method and discusses the change in mechanical properties of reinforced sand. Such a research attempt will provide some reference frame for its practical engineering applications.

Material and methods

Material

Sand

The sand used in this study was singled out from Nanjing city, China. The sand sample and particle size distribution of sand are shown in Fig. 1. The maximum dry density (ρ_{max}) and the minimum dry density (ρ_{min}) of sand are 1.66 g/cm^3 and 1.34 g/cm^3 respectively. The maximum void ratio (e_{max}) and the minimum void ratio (e_{min}) are 0.97 and 0.59 respectively. The specific gravity (G_s) of 2.65, the gradation coefficient (C_g) of 1.13, and the uniformity coefficient (C_u) of 2.77 are also observed. The sand particles have a mean grain size (D_{50}) of 0.30 mm. These basic physical parameters of sand are given in Table 1. The sand used for the present experimental program was crushed, dried, and then sieved with a 2-mm sieve.

Fibers

As a kind of non-artificial fiber, sisal fiber (as shown in Fig. 2a) is an economic material with rough surface, high hardness, elasticity, and tensile strength. Its breaking tensile strength and Young's modulus are about 450–700 MPa and 7–13 GPa respectively. Palm fiber (as shown in Fig. 2b) as a non-artificial fiber has similar rough surface as sisal fiber, but its hardness, elasticity, and tensile strength are weaker than those of sisal fiber. Its breaking tensile strength and Young's modulus are about 87 MPa and 0.63 GPa respectively. Polypropylene fiber (as shown in Fig. 2c) as the artificial fiber is a white material with smooth surface, high strength, high elasticity, high toughness, wear resistance, and corrosion resistance. Its breaking tensile strength and Young's modulus are about 358 MPa and 3.5 GPa respectively. The length of all three fibers was set to 18 mm and the content of each type of fiber was set to 0.8%. The fiber content in this present research was defined as the weight ratio of fiber to dry sand, which can be calculated as the following:

$$C_f = \frac{M_f}{M_s} \quad (1)$$

where C_f(%) is defined as the fiber content, M_f(g) is the weight of the used fiber, and M_s (g) is the weight of the dry sand.

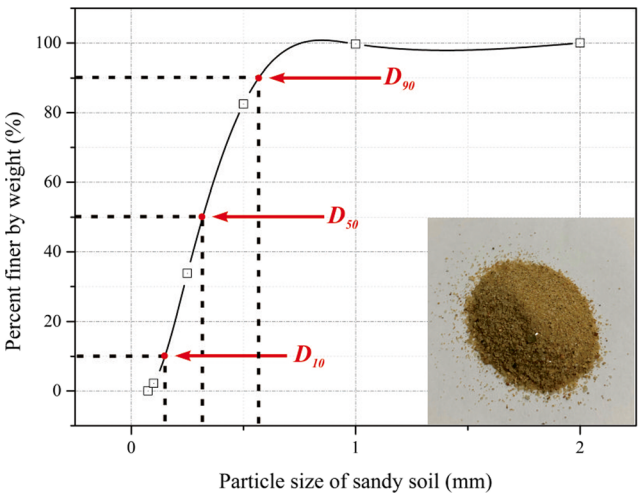

Fig. 1 Distribution particle size of sand

Table 1 Physical behaviors of the test sand

ρ_{max} (g/cm^3)	ρ_{min} (g/cm^3)	e_{max}	e_{min}	G_s	C_g	C_u	D_{50} (mm)
1.66	1.34	0.97	0.59	2.65	1.13	2.77	0.30

Polyurethane organic polymer

The sand solidification agent used in this study is a polyurethane organic polymer and it can form reticulated membrane after coming in contact with water. This polymer has some unique properties such as well flexibility, excellent elasticity, aging resistance, and outstanding adaptability in the environment of high-low temperatures. Additionally, due to the presence of hydrophilic polyurethane in polymer, it is convenient to be used in construction and contributes towards cost reduction. The preparation process of polymer is discussed in the following steps.

Firstly, 50 g each of polypropylene glycol (abbreviated as PPG2000) and polyoxyethylene glycol (abbreviated as PEG2000) with the number average molecular weight of 2000, 20 g polycaprolaclone glycol (abbreviated as PCL1000) with the number average molecular weight of 1000 and 200 ml toluene were placed in the reaction vessel (a flask with three necks). It was then stirred evenly after heating to 145 °C. After complete melting of the polymer polyol, it was then subjected to atmospheric distillation. When the toluene was nearly evaporated to dryness, it was switched over to vacuum distillation until the residual moisture and toluene in the system were completely removed. Secondly, the temperature was lowered to room temperature and the pressure-reducing device was removed. Then, nitrogen was introduced and the reaction system was oil sealed after placing the reflux condenser. Afterwards, 20 g toluene diisocyanate (abbreviated as TDI) was added into the reaction vessel and stirred evenly with heating at 90 °C temperature for 2 h. Finally, 200 ml ethyl acetate (abbreviated as EA) was added into the reaction vessel and stirred for 1 h evenly after cooling the system to normal temperature. Thus, the preparation of the polymer was completed. It was then sealed and stored for use. The finished product of polymer and schematic diagram of its molecular formula are shown in Fig. 3.

Suzhou Bo Chang Chemical Co., Ltd., Suzhou, China, supplied all the chemicals used in this process.

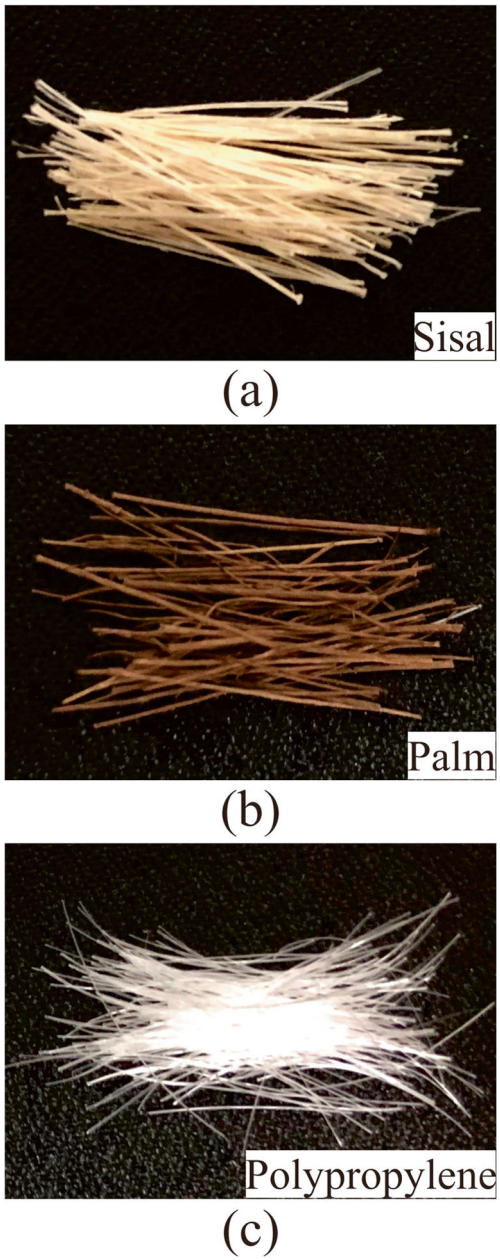

Fig. 2 The pictures of three kinds of fiber: **a** sisal fiber; **b** palm fiber; **c** polypropylene fiber

Methods

To understand the influence of dry density (D_d), polymer concentration (C_p), and fiber type on the tensile strength, unconfined compression strength and tension-compression ratio of reinforced sand, direct tensile, and unconfined compression tests are designed. Dry sand density, polymer concentration, and fiber types were varied, whereas the moisture content was kept constant at 10%. Polymer concentration was set to 2% and the dry sand densities were set to 1.4 g/cm^3, 1.5 g/cm^3, and 1.6 g/cm^3 respectively. For density of 1.5 g/cm^3, the different fiber combinations and polymer concentrations (C_p of 1%, 2%, and 3%) were investigated. In total, 36 groups of samples (i.e., 18 sets of tensile samples and 18 sets of compression samples) were prepared. The water content and polymer concentration in this study were defined as the weight ratio of water to dry sand and the weight ratio of polymer to dry sand respectively as per the following:

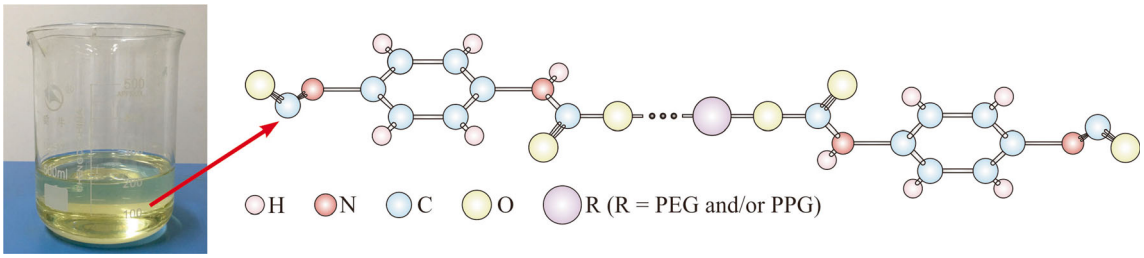

Fig. 3 The picture of polyurethane organic polymer

$$C_w = \frac{M_w}{M_s} \quad (2)$$

$$C_p = \frac{M_p}{M_s} \quad (3)$$

where C_w (%) is defined as the water content, M_w (g) is the weight of the water, C_p (%) is defined as the polymer concentration, M_p (g) is the weight of the polymer, and M_s is the weight of the dry sand.

Unconfined compressive test

For unconfined compressive tests, the samples were prepared with a height of 80 mm and diameter of 39.1 mm. They are formed with a static compaction method as per ASTM D2166. For the sample with sisal-palm fiber combination, polymer concentration of 2% and sample density of 1.5 g/cm^3 are used as a demo. According to the stipulation of the previous test scheme, the corresponding weights of sisal fiber, palm fiber, and sand are measured, fully mixed, and set aside. Subsequently, the polymer with a concentration of 2% is weighed and mixed with water. Then, the polymer solution is mixed with fiber-sand mixture immediately in order to prevent the solidification of polymer into membrane in contact with water. Finally, the resulting mixture is evenly poured into the corresponding molds, pressed with a jack, and kept for 2 min before being taken out. The prepared compressive sample is shown in Fig. 4 a. The samples are then placed in a constant room temperature to cure for 48 h before the test.

In the unconfined compressive test, the prepared sample is placed in the YYW-2 strain control type unconfined pressure gauge (manufactured by Nanjing Sand Instrument Factory Co. Ltd) as shown in Fig. 5. It controls the rate of the pressure gauge by lifting the plate of the unconfined pressure gauge at a controlled rate of 2.4 mm/min. In addition, the sample reaches the peak compressive strength at an axial strain of 10% approximately. In order to further explore the subsequent changes in the sample, the compressive test was continued up to an axial strain of about 25%. The failure pattern of the sample is shown in Fig. 4 b. Finally, the stress-strain curve of the corresponding sample is recorded for analysis of compressive mechanical properties.

Direct tensile test

For the direct tensile test, the samples were prepared with a height of 25 mm and basal area of 4200 mm^2. They are made with the static compaction method as per ASTM D2166. The process of preparation of tensile sample is exactly the same as

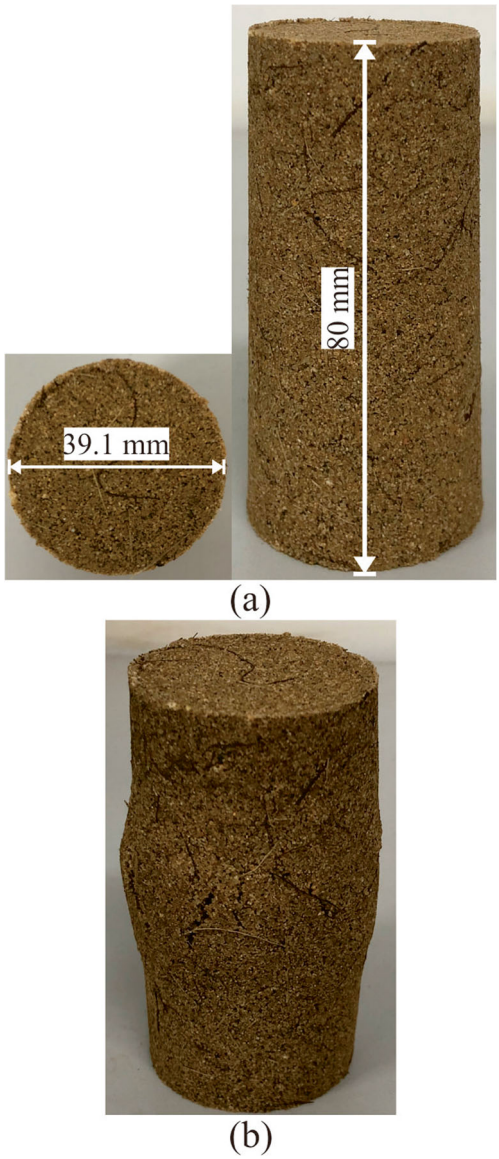

Fig. 4 The pictures of finished and damaged compressive sample: **a** finished compressive sample; **b** damaged compressive sample

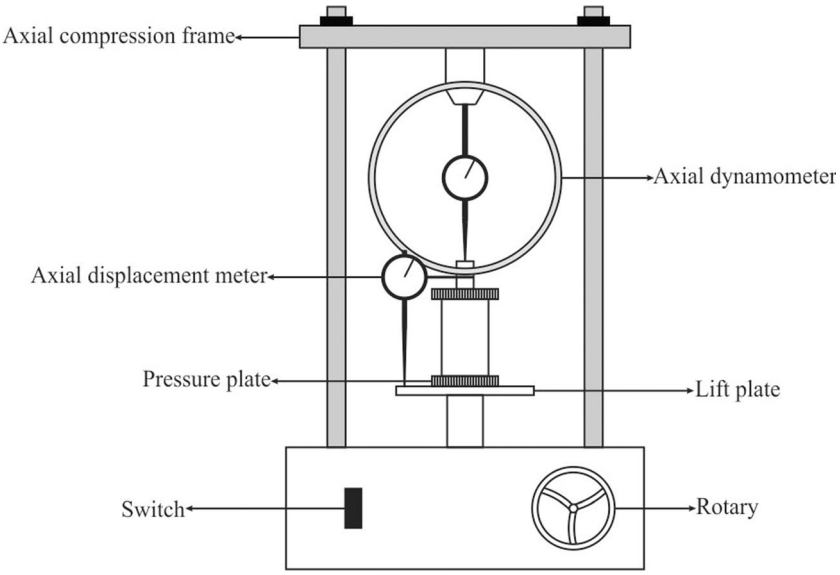

Fig. 5 The picture of YYW-2 strain control type unconfined pressure gauge

that of compression sample except the types of molds. A tensile sample thus prepared is shown in Fig. 6 a.

The prepared sample is placed in a tensile tester (manufactured by Nanjing Sand Instrument Factory Co. Ltd) as shown in Fig. 7. In case of all the tensile tests, the test process is terminated as and when the middle section of the sample is disconnected. An example of the failed sample is shown in Fig. 6 b. The tensile strength obtained at the sample failure is recorded. As the termination of the tensile test is defined as the sample being disconnected, the displacement in the sample during the test is not obvious.

Results and discussions

Based on the results of the above two tests, the tension-compression ratio (B_r) in addition to the compressive and tensile strengths of the samples is considered as a reference to evaluate the mechanical property of the reinforced sand, which can be calculated as the following:

$$B_r = \frac{\sigma_t}{\sigma_c} \tag{4}$$

where B_r is defined as the tension-compression ratio, σ_t is the breaking tensile strength, and σ_c is the peak compressive strength.

Meanwhile, scanning electron microscopic analysis for representative samples from the unconfined compressive and direct tensile tests was done to analyze the strengthening mechanism of the reinforced sand. And in order to make the results and discussion more accurate and intuitive, the reference frame of 2% polymer concentration and 1.5 g/cm^3 density in the test program will be used for the following discussions.

Effect of the change in density, polymer concentration, and fiber combination on tensile strength

As seen in Fig. 8 a, the tensile strength increased with increasing density of samples with the same fiber combination and

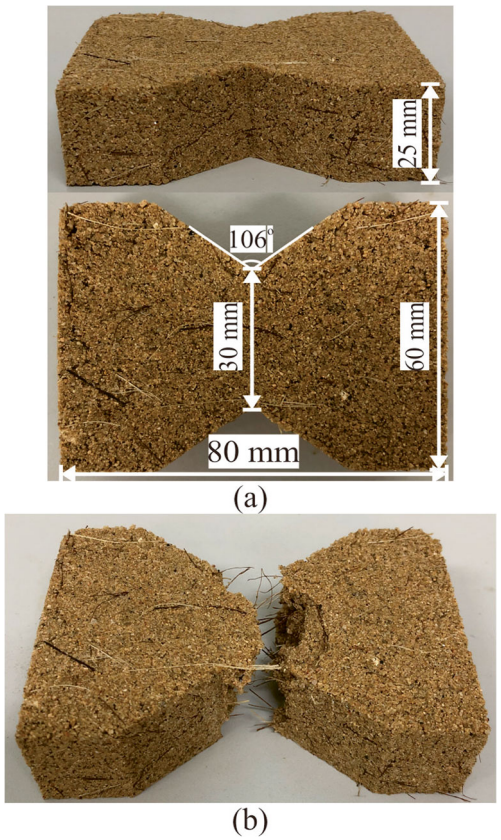

Fig. 6 The pictures of finished and damaged tensile sample: **a** finished tensile sample; **b** damaged tensile sample

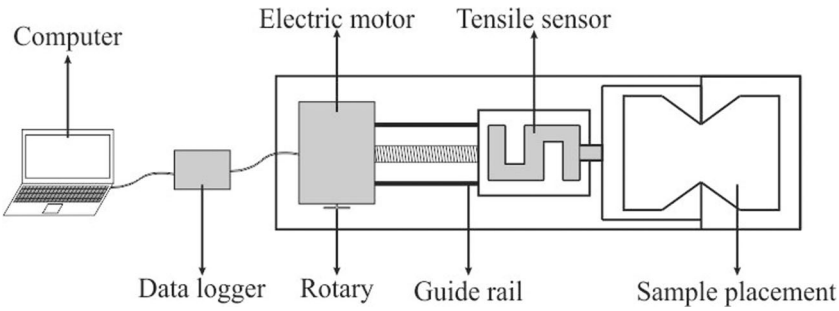

Fig. 7 The picture of tensile tester

polymer concentration of 2%. The reason for such result may be attributed to the fact that with greater density of the sample, the contact between the sand particles and fibers became closer as compared with that in case of lesser density sample. The reticulated membrane envelops the sand particles with the fibers. By observing the three curves in Fig. 8 a, it can be stated that the trends of the curves for palm-polypropylene and sisal-polypropylene fiber combinations were relatively stable with linear changes. Conversely, the tendency of the curve for sisal-palm fiber combination was comparatively flatter in the range of 1.4–1.5 g/cm^3, and it became steep suddenly in the range of 1.5–1.6 g/cm^3. The reason for this may be due to a more rough surface of non-artificial fibers (sisal and palm) compared with polypropylene fibers (i.e., artificial fibers). Hence, the two non-artificial fibers will have a better tensile effect after winding and warping. The difference between the maximum and minimum tensile strengths on the curve of sisal and palm fibers was about 13.03 kPa. At the same time, it can be clearly observed by longitudinally comparing the curves in Fig. 8 a that the tensile strength of sample with palm-polypropylene fibers was generally greater than that of the other two. This fully demonstrates that the addition of palm and polypropylene fibers to the sample can exert a better tensile effect at the same density and the maximum tensile strengths were 151.97 kPa, 157.77 kPa, and 162.96 kPa for densities of 1.4 g/cm^3, 1.5 g/cm^3, and 1.6 g/cm^3 respectively (as can be seen from Fig. 8b). The tensile strength values of the samples with different fiber combinations have no significant differences in case of 1% polymer concentration, but the differences in tensile strengths for three different fiber combinations were gradually revealed for 2% and 3% polymer concentrations. It can be seen from the analysis that this difference was the embodiment of suitability of different fiber combinations for the tensile strength of the sample with increasing polymer concentration. When the concentration of the polymer was less (i.e., 1%), the fibers could not be sufficiently wrapped and thus the reinforcing effect was not fully exerted due to the formation of less reticulated membrane inside the sample. Although the differences between the three were not significant, it can still be seen that the addition of palm and polypropylene fibers was the best effective one. Inversely, with the increase in polymer concentration, the formation of reticulated membrane increases and the suitability of fiber reinforcement is gradually reflected. As seen in the Fig. 8 b, the differences between the maximum and minimum tensile

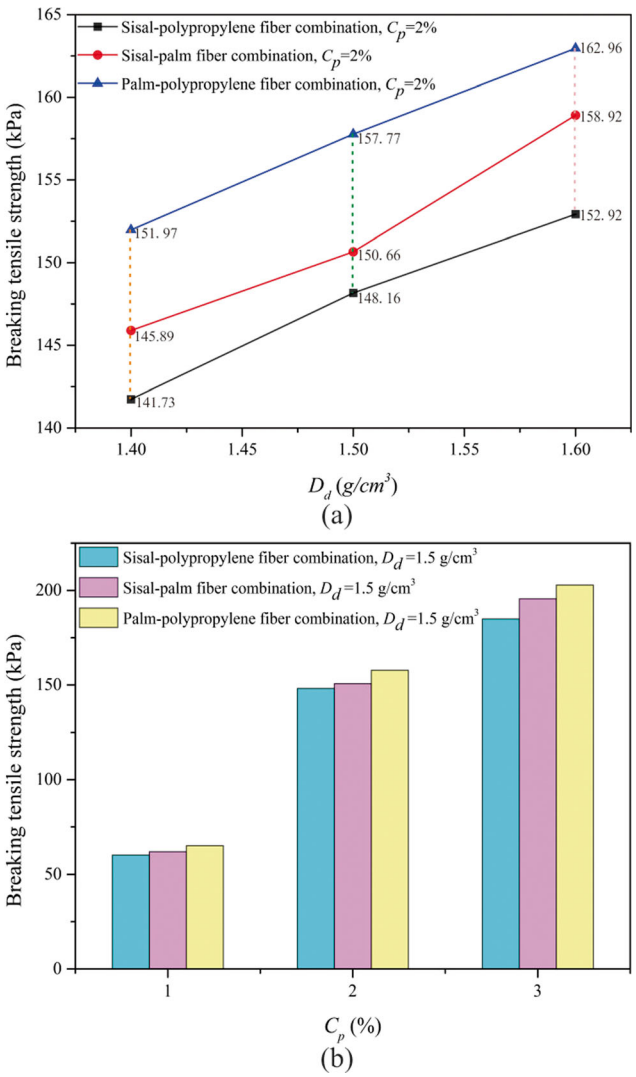

Fig. 8 The comparison of peak tensile strength of samples with the different density, polymer concentration, and fiber combination: **a** the density is fixed while the polymer concentration and the fiber combinations are changed; **b** the polymer concentration is fixed while the density and the fiber combinations are changed

strengths at 1%, 2%, and 3% C_p were 5.04 kPa, 9.61 kPa, and 18.00 kPa respectively.

Effect of the change in density, polymer concentration, and fiber combination on compressive strength

The test data comparison of the same and different fiber combinations was performed for better analysis. Figure 9 a, b, and c show the comparison between the stress-strain curves of samples with the same density and fiber combination, and different polymer concentrations, whereas Fig. 10 a, b, and c display the stress-strain curves of samples with different fiber combinations and same polymer concentration and density. All the samples displayed the behavior of strain-softening ductile failure. As seen in Fig. 9 a, b, and c for all the three different fiber combinations, the stress-strain curves of all the samples show similar trends and the axial stress increases with the increase in density. Similar to the influence of density on the tensile strength of the reinforced sand, it also has a significant influence on the compressive strength of the sample and presents a positive correlation. It was also found that there was no significant decrease in compressive strength after reaching its peak, but it remains stable or slightly increased as observed in Fig. 9. It can be inferred that the significant supporting effect was generated inside the sample after addition of fiber due to friction and occlusion between fiber and sand, even though the sample was damaged eventually. In addition, it can be further observed that the tensile strength of the sample with the addition of palm and polypropylene fibers shows a certain degree of rise after reaching the peak value (Fig. 9c). This is because of the fact that the reinforced sample does not experience a fracture failure. The middle part of the failed sample is observed to be slightly protruding, while the two ends remained undisturbed (as shown in Fig. 4b). This may be due to the random structural reorganization of the fibers inside the sample. According to the comparison between the peak compressive strengths of three different fiber combination cases (Fig. 10a–c), the curves of sisal-polypropylene, palm-polypropylene, and sisal-palm fiber combinations display a descending order. Compared with Fig. 10 a, the intersections of the curves in Fig. 10 b and c were witnessed after reaching the peak value of the compressive strength and the axial strain was about 0.18 at this time. This indicates that the addition of palm and polypropylene fibers to the sample was quite helpful in the reorganization of its internal structure after destruction. In addition, the stress-strain curves of the sample containing sisal and polypropylene fibers and containing palm and polypropylene fibers were observed to be quite similar with increasing density (Fig. 10b and c). However, the stress-strain curves of the sample containing sisal and palm fibers were significantly different from the other two cases.

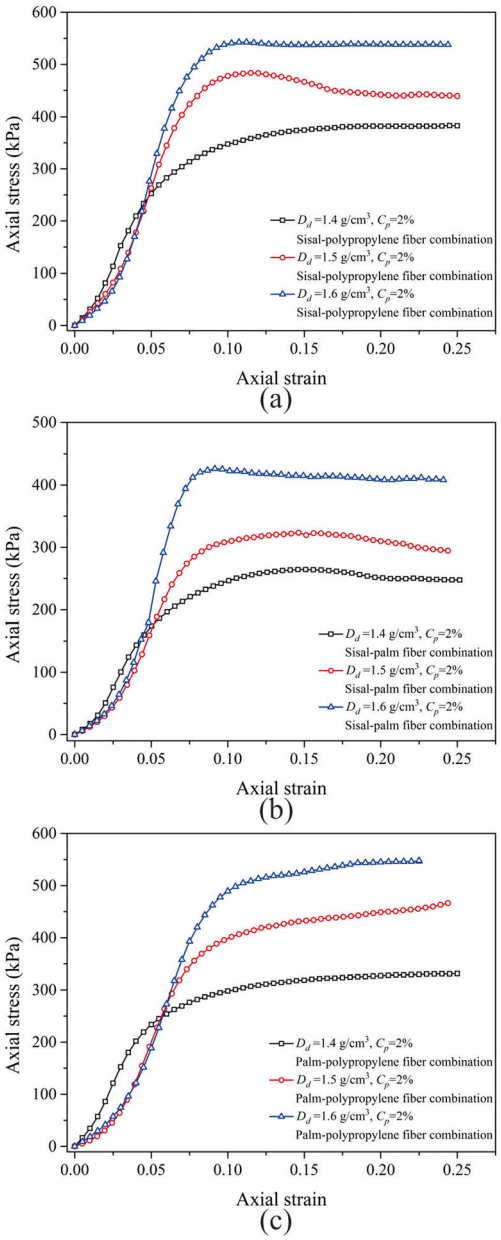

Fig. 9 The comparison of axial stress of samples with the same fiber combination and polymer concentration, and the different density: **a** fiber combination: sisal-polypropylene fiber combination; **b** fiber combination: sisal-palm fiber combination; **c** fiber combination: palm-polypropylene fiber combination

Figure 11 a, b, and c display the test results of the compressive strengths of the samples with the same fiber combination and density, and with different contents of polymer concentration. It was observed that the change in compressive strength of the samples has the same regularity as described above and the magnitude of increase was significant as compared with previous results. The differences between maximum and minimum peak compressive strengths in Fig. 11 a, b, and c were 299.99 kPa, 226.72 kPa, and 301.12 kPa, respectively. Furthermore,

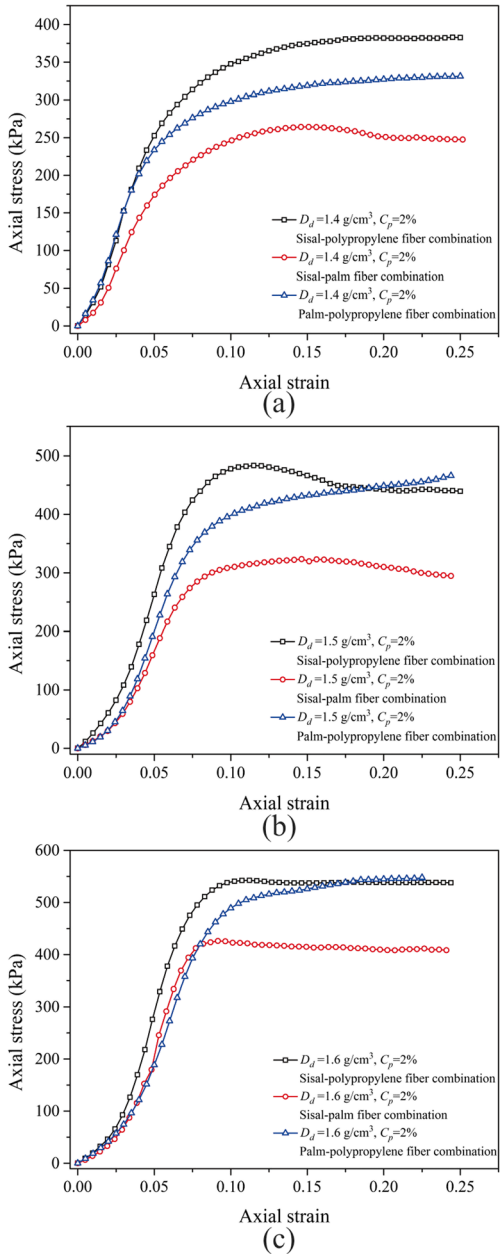

Fig. 10 The comparison of axial stress of samples with the same polymer concentration and density, and the different fiber combination: **a** density is 1.4 g/cm^3, polymer concentration is 2%; **b** density is 1.5 g/cm^3, polymer concentration is 2%; **c** density is 1.6 g/cm^3, polymer concentration is 2%

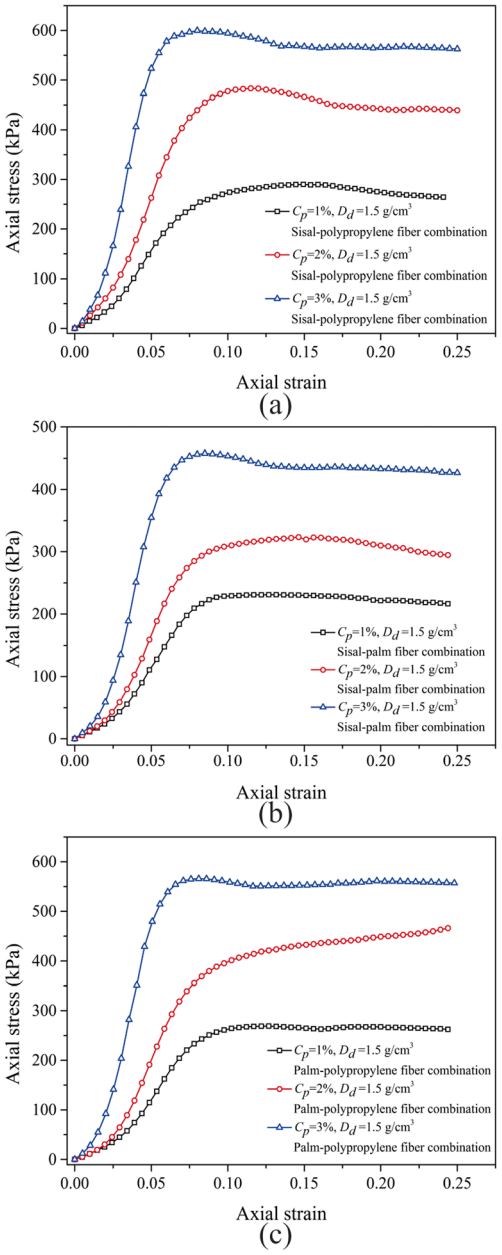

Fig. 11 The comparison of axial stress of samples with the same fiber combination and density, and the different polymer concentration: **a** fiber combination: sisal-polypropylene fiber combination; **b** fiber combination: sisal-palm fiber combination; **c** fiber combination: palm-polypropylene fiber combination

as seen in Fig. 12 a, b, and c, the stress-strain curve of sisal and polypropylene fibers has a similar trend with that of palm and polypropylene fibers, and as a whole, there was not much difference in the compressive strength. This shows that the sisal and polypropylene fibers, as well as palm and polypropylene fibers, have similar ability to recombine the internal structure of the damaged sample and the recombination was made after being bound and entangled by the reticulated membrane formed by polymer. Particularly, the curve for sisal and polypropylene fibers and the curve for palm and polypropylene fibers in Fig. 12 a, b, and c show a certain degree of overlap at the end, which was most evident in Figs. 12 a and c. However, although the recombination ability was similar, the former was slightly stronger. The differences between the peak compressive strengths between the two were 25.29 kPa, 50.77 kPa, and 24.04 kPa for 1%, 2%, and 3% contents of polymer concentration respectively. In contrast, the peak compressive strength of the sample containing sisal and palm fibers was significantly lower than the previous two

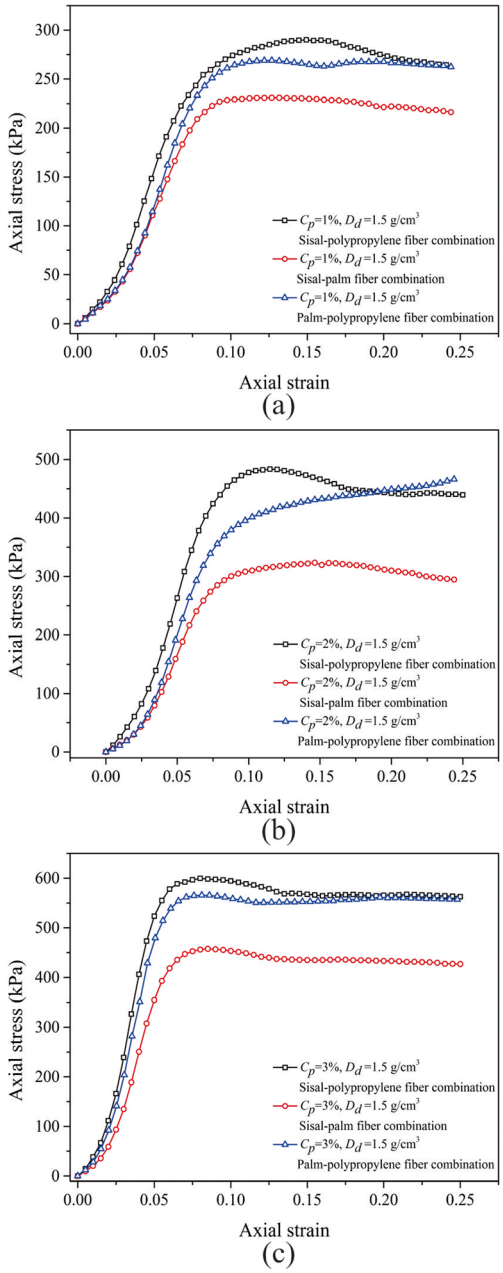

Fig. 12 The comparison of axial stress of samples with the same polymer concentration and density, and the different fiber combination: **a** polymer concentration is 1%, density is 1.5 g/cm^3; **b** polymer concentration is 2%, density is 1.5 g/cm^3; **c** polymer concentration is 3%, density is 1.5 g/cm^3

cases, and the most prominent differences in peak compressive strengths were approximately 159.99 kPa and 109.22 kPa, respectively (Fig. 12b).

Effect of the change of density, polymer concentration, and fiber combination on tension-compression ratio

The peak compressive strength and breaking tensile strength of the samples with 2% contents of polymer concentration and at 1.4 g/cm^3, 1.5 g/cm^3, and 1.6 g/cm^3 densities are listed in Table 2. In addition, the tension-compression ratio (B_r) of peak compressive strength and breaking tensile strength is also listed in the table. The change in compressive and tensile strengths of the samples can be seen from Table 2 and it was observed that these values increase with increasing density, as has already been discussed in the previous section. The tension-compression ratio (Table 2) was also shown as curves in Fig. 13 a. It can be inferred that the change in the tension-compression ratio of the reinforced sand varies with the density and fiber combination. As seen in Fig. 13 a, the tension-compression ratio of reinforced sand with different fiber combinations gets reduced with increasing density. This curve for sisal and palm fibers decreases linearly with increasing density. However, the curves for other two fiber combinations decrease rapidly within the range of 1.4–1.5 g/cm^3 density and then decrease slowly within the range of 1.5–1.6 g/cm^3. The tension-compression ratio values of the three fiber combinations were observed to be the smallest and closest to each other at a density of 1.6 g/cm^3 and the corresponding values for sisal-palm, palm-polypropylene, and sisal-polypropylene fiber combinations were 0.373, 0.309, and 0.282 respectively. Further, the trend from highest to lowest tension-compression ratio at each density value was observed in the order of sisal-palm, palm-polypropylene, and sisal-polypropylene fiber combinations. From the above analysis, it may be concluded that the greater is the density of the reinforced sand, the smaller will be the tension-compression ratio. The tension-compression ratio is observed to be the maximum for sisal-palm fiber combination and minimum for sisal-polypropylene fiber combination.

The peak compressive strength, breaking tensile strength, and tension-compression ratio of the samples with 1.5 g/cm^3 density and 1%, 2%, and 3% contents of polymer concentration are listed in Table 3. The tension-compression ratio as listed in Table 3 was also shown in the Fig. 13 a and b. By comparing the curves in the Fig. 13 b, the tension-compression ratio values were 0.269, 0.246, and 0.223 for sisal-palm, palm-polypropylene, and sisal-polypropylene fiber combinations respectively and were observed to be minimum at 1% polymer concentration. The tension-compression ratio increased significantly within the range of 1 to 2% polymer concentration and was most prominent in case of sisal-palm fiber combination. Except for slight increase in the tension-compression ratio in case of sisal-polypropylene fiber combination, the ratio values for other two fiber combinations decreased slightly within the range of 2 to 3% polymer concentration. It can thus be inferred that the content of polymer concentration should be 1% approximately for strengthening the sand using polymer and fiber combinations. It was also observed from Fig. 13 a and b that the tension-compression ratio values of the sample with sisal-palm fiber combination were the largest of the three combinations at the same density

Table 2 The tension-compression ratio of samples with the different fiber combination and density, and the same polymer concentration

Fiber combination	Sisal-polypropylene fiber combination			Sisal-palm fiber combination			Palm-polypropylene fiber combination		
Polymer Concentration (%)	2	2	2	2	2	2	2	2	2
Density (g/cm^3)	1.4	1.5	1.6	1.4	1.5	1.6	1.4	1.5	1.6
Peak compressive strength (kPa)	374.5	483.4	542.5	264.2	323.4	426.1	320.4	432.7	525.9
Breaking tensile strength (kPa)	141.7	148.2	152.9	145.9	150.7	158.9	151.9	157.8	162.9
Tension-compression ratio	0.378	0.308	0.282	0.552	0.466	0.373	0.474	0.365	0.309

and polymer concentration and the maximum value reached to about 0.552 at 1.40 g/cm^3 density and 0.466 at 2% contents of polymer concentration. When polymer concentration increased from 1 to 2%, the tension-compression ratio of the three samples demonstrated a huge increase. Meanwhile, the changes in tension-compression ratios for different fiber combinations remained the same.

Mechanism analysis

The polyurethane organic polymer as a water-soluble sand solidification agent was thoroughly mixed with water and added to the fiber-reinforced sand with proper stirring. A series of physical reactions occurred between the sand particles and the three kinds of fiber combinations, and thus formed a certain reticulated membrane structure with elasticity and glutinousness by mutual diffusion, penetration, and entanglement (Fig. 14). This reticulated membrane structure helped in close bonding between the sand particles that were originally loose. Meanwhile, the pores between the sand particles were also sufficiently filled so that the reinforced sand becomes more compact and harder material due to the existence of the reticulated membrane. As shown in Figs. 8 b and 11, the tensile and compressive strengths of the samples increased with increasing content of polymer concentration while adding the same combination of reinforcing fibers.

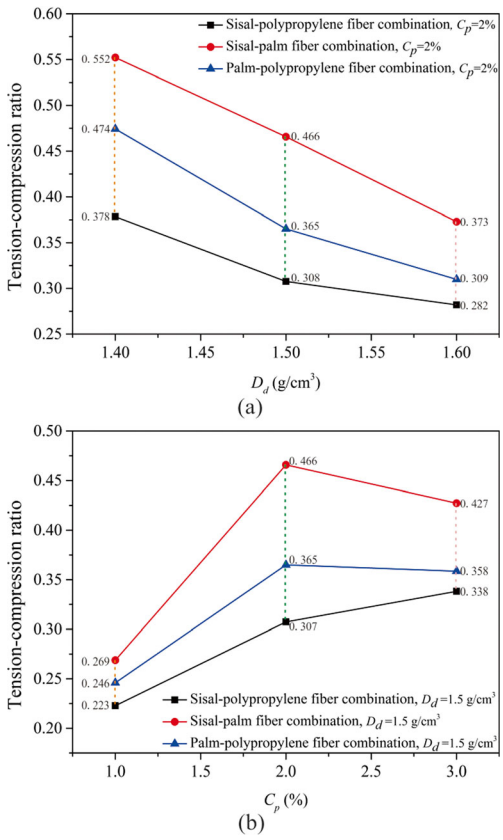

Fig. 13 The picture of tension-compression ratio of the sample: **a** the sample with the different fiber combination and density, and the same polymer concentration; **b** the sample with the different fiber combination and polymer concentration, and the same density

As the content of polymer concentration increased with almost constant sample density, the volume of reticulated membrane structure formed by mixing the polymer with water between the sand particles increased in approximately equal space (Fig. 15). Furthermore, the porosity in the space between the sand particles decreased with gradual increase in sample density. In the process, the reticulated membrane structure and the sand particles became more compact, thereby increased the effective contact area (as shown in Fig. 16) and the frictional resistance between each other.

In addition to polymer, the tensile and compressive strengths can be further improved by adding fibers to the sand. Therefore, the sisal, polypropylene, and palm fibers in combination of any two were selected in this present study. The breaking tensile strengths of these fibers in descending order are observed as sisal fiber, polypropylene fiber, and palm fiber. The stiffness of the sisal fiber was the largest and had rough surface, while the polypropylene fiber was the softest with best toughness and smooth surface. From the results of the tensile tests, it was observed that the sample with palm-polypropylene fiber combination has the largest breaking tensile strength, while the sample with sisal-polypropylene fiber combination has the smallest, even with the changing polymer concentration and density. Although the sisal fiber has the greatest tensile strength, it was pulled out from the sand particles without reaching the upper limit of the pulling force (the sisal fiber gets broken) due to its excessive rigidity. And it was largely dependent on the junction between the polypropylene fiber and the sand particles to counteract the tensile force. In

Table 3 The tension-compression ratio of samples with the different fiber combination and polymer concentration, and the same density

Fiber combination	Sisal-polypropylene fiber combination			Sisal-palm fiber combination			Palm-polypropylene fiber combination		
Density (g/cm^3)	1.5	1.5	1.5	1.5	1.5	1.5	1.5	1.5	1.5
Polymer concentration (%)	1	2	3	1	2	3	1	2	3
Peak compressive strength (kPa)	290.1	483.4	589.9	230.9	323.4	457.7	264.8	483.4	565.9
Breaking tensile strength (kPa)	64.6	148.2	199.5	62.1	150.7	195.5	65.1	157.8	202.9
Tension-compression ratio	0.223	0.307	0.338	0.269	0.466	0.427	0.246	0.365	0.358

contrast, although the palm fiber has a small tensile strength, it could withstand the pulling force as far as possible due to its moderate rigidity and being twined and wrapped by polypropylene fiber. Hence, this palm-polypropylene fiber combination achieved the maximum tensile strength. This mechanism can be more clearly understood by comparing Fig. 17 a and b. In the compression test, the sample with sisal-polypropylene fiber combination can withstand the highest compressive strength, while the sample with sisal-palm fiber combination has its smallest value. Obviously, sisal fiber was the hardest of the three as mentioned above. Therefore, not only the advantage of its own hardness could be fully utilized but also the toughness of sisal fiber got improved under the wrapping and twining of the polypropylene fiber. Therefore, the stability of sand particles could be further enhanced in the process of resisting the compression. Moreover, since the hardness of palm fiber was slightly worse than that of sisal fiber, although it was also twined by polypropylene fiber, the anti-compression effect of the palm-polypropylene fiber combination was slightly worse in comparison with that of the sisal-polypropylene fiber combination. In addition, the sisal-palm

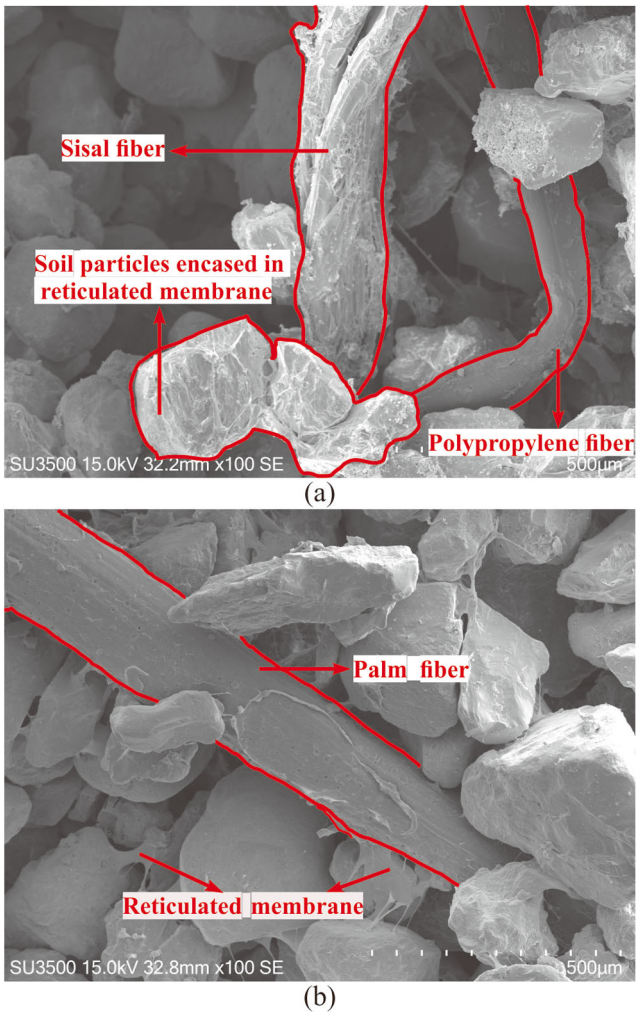

Fig. 14 The scanning electron microscopy micrographs (100 times magnification) of reinforced sand: **a** sisal fiber; **b** palm fiber

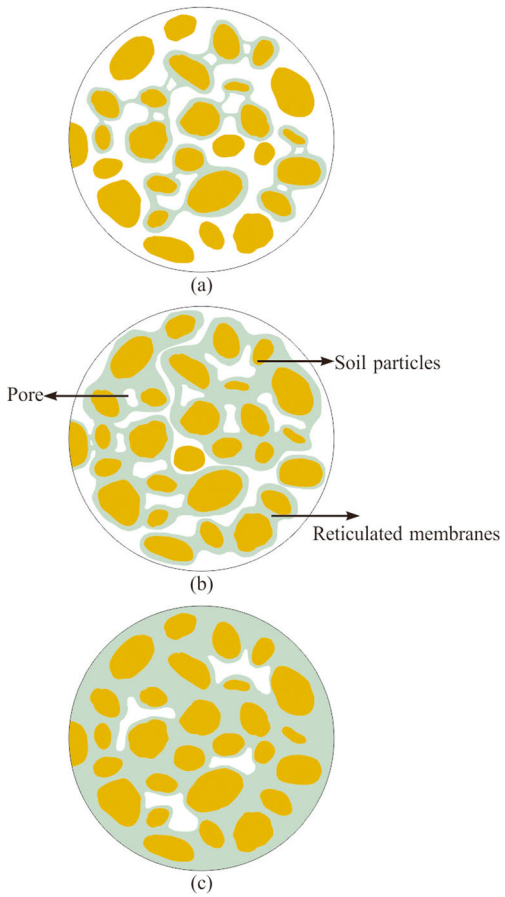

Fig. 15 The reinforced schematic diagram of the different polymer concentration: **a** light polymer concentration; **b** medium polymer concentration; **c** high polymer concentration

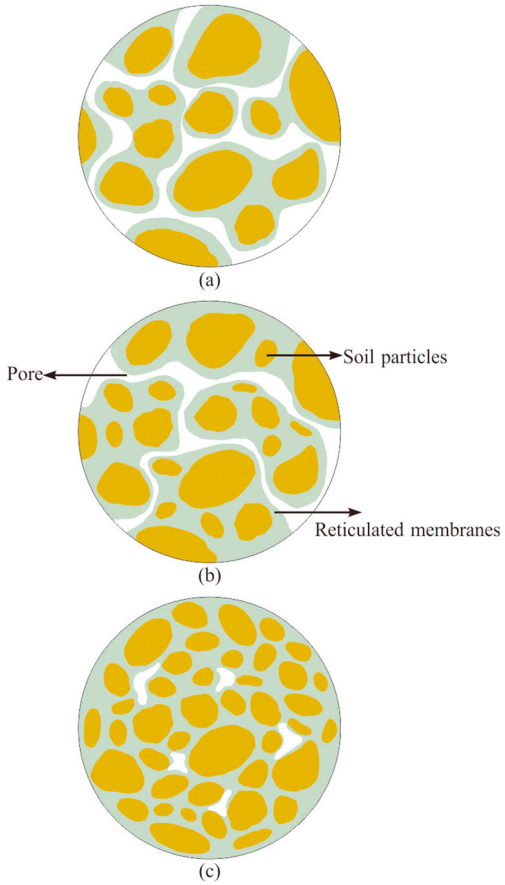

Fig. 16 The reinforced schematic diagram of the different density: **a** low density; **b** medium density; **c** high density

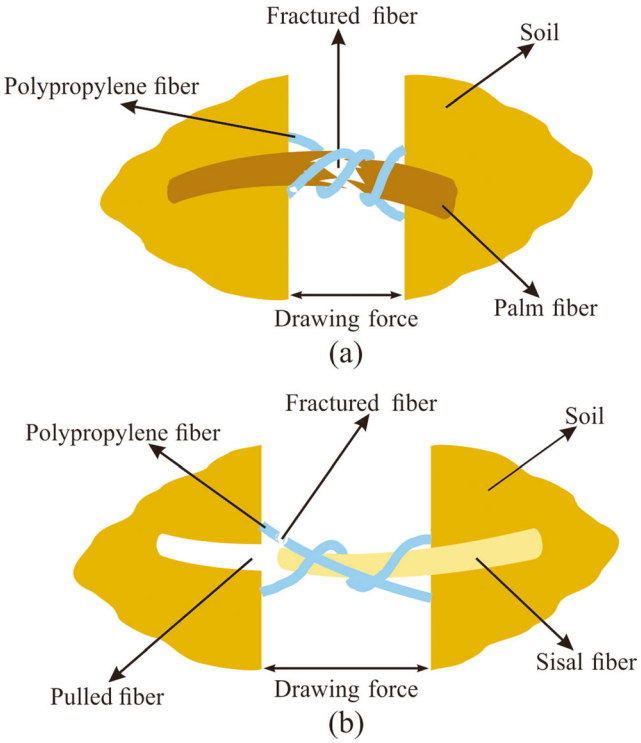

Fig. 17 The drawing schematic diagram of the different fiber combination: **a** fiber combination: palm-polypropylene fiber combination; **b** fiber combination: sisal-polypropylene fiber combination

fiber combination without polypropylene fiber twining showed the worst compressional effect.

The tension-compression ratio of reinforced sand could be calculated using Formula (4) by substituting the data obtained from the tensile and compressive tests. And, the decreasing order of fibers in terms of tension-compression ratio of samples was observed to be sisal-palm, palm-polypropylene, and sisal-polypropylene irrespective of the change in polymer concentration and density values. The degree of irregularity in which the fracture in the sample was broken can be used as a basis for evaluating the ability of resistance to damage during the tensile process. As seen in Fig. 18 a, the cross section of the fracture in the broken sample was relatively flat and damaged in case of polypropylene fibers and relatively undamaged in case of sisal fibers showing weaker ability to resist damage. The sample in Fig. 18 b was observed to have an uneven cross section as compared with the former one and shows improved ability to resist damage. Conversely, in case of sisal-palm fiber combination as shown in Fig. 18 c, the sand particles near the cross section appear partially displaced when the sample was unbroken. This was because the high-hardness sisal and palm fibers were pulled out from the sand particles, and under the winding and warping of the reticulated membrane structure, some sand blocks were pulled following the homeopathic direction jointly. Thus, the extremely uneven cross section was produced. Therefore, the ability to resist damage of the sample with sisal-palm fiber combination was the best. Furthermore, the fiber has the function of supporting the sand particles, and there was occlusion effect within the sand particles, which can effectively slow the occurrence of the deformation and inhibit the damage in the sample to a certain extent when the sample was subjected to pressure. It can be seen that even after reaching the peak compressive strength, the strength of the sample did not decrease immediately. But, there was a buffer period to reorganize the internal structure, and the compressive strength may even continue to rise.

At present, the technology has been applied to the reinforcement of the riverbank slopes in Jiangsu Province, China, and preliminary results are obtained. The original loose sandy slope has been improved and the overall structure has been enhanced, which can effectively resist erosion. Detailed results will be introduced in subsequent studies.

Conclusions

In this present work, a series of laboratory tests were carried out to verify some effects of different polymer concentrations, dry densities, and fiber combinations on the mechanical properties of the reinforced sand. Furthermore, the failure

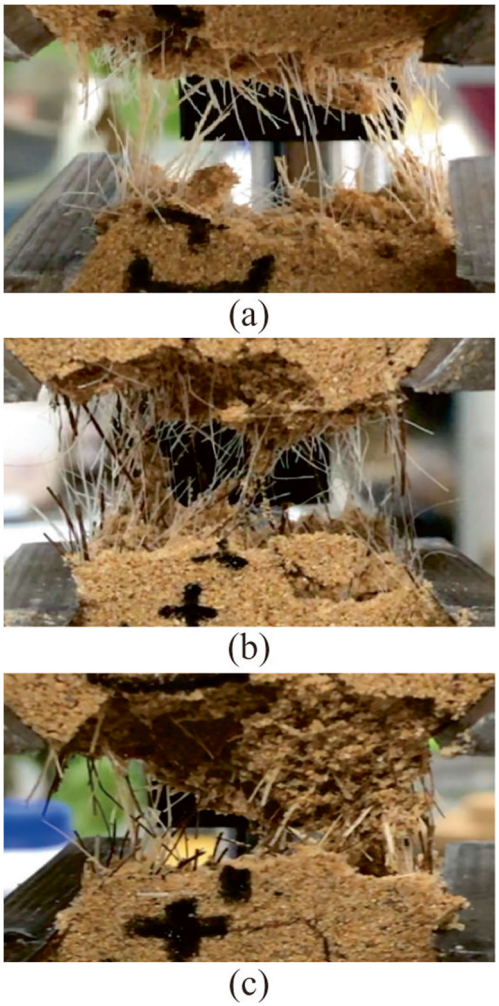

Fig. 18 The drawing fracture section diagram of the different fiber combination: **a** fiber combination: sisal-polypropylene fiber combination; **b** fiber combination: palm-polypropylene fiber combination; **c** fiber combination: sisal-palm fiber combination

mechanism of the reinforced sand was analyzed from the photomicrographs of scanning electron microscopy. The results of the study can be summarized as follows:

1. Both tensile and compressive strengths increase with increasing sample density and polymer concentration. Maximum tensile and compressive strengths are observed to be 162.9 kPa (for 1.6 g/cm^3 sample density and palm-polypropylene fiber combination) and 542.5 kPa (for 1.6 g/cm^3 sample density and sisal-polypropylene fiber combination) respectively for 2% polymer concentration. For 1.5 g/cm^3 density, the maximum tensile and compressive strengths are observed to be 202.9 kPa (for 3% polymer concentration and palm-polypropylene fiber combination) and 589.9 kPa (for 3% polymer concentration and sisal-polypropylene fiber combination) respectively.
2. With constant polymer concentration and increasing sample density, the variation in tension-compression ratio for different fiber combinations ranges as follows: 0.373–0.552 for sisal-palm fiber combination, 0.309–0.474 for palm-polypropylene fiber combination, and 0.282–0.378 for sisal-polypropylene fiber combination. For the same sample density and increasing polymer concentration, the variation in tension-compression ratio for different fiber combinations ranges as follows: 0.269–0.466 for sisal-palm fiber combination, 0.246–0.365 for palm-polypropylene fiber combination, and 0.223–0.338 for sisal-polypropylene fiber combination.
3. Based on the observation from scanning electron microscopic studies, the reticulated membrane has been found as a bridge to produce the excellent cementation between the sand particles and the fibers. The overall structure and strength of sand have been effectively improved. Furthermore, by combining the above conclusions, it can be stated that different fiber combinations, dry densities, and polymer concentrations have different reinforcement effects on sand. The present attempt provides some reference frame for hybrid fiber polymer-based sand reinforcement for its future practical engineering applications.

Funding information This research was financially supported by Fundamental Research Funds for the Central Universities (Grant No. 2019B77514) and Postgraduate Research & Practice Innovation Program of Jiangsu Province (Grant No. SJCX19_0153), and National Natural Science Foundation of China (Grant No. 41877212).

References

Anamica, Pande PP (2018) Synthesis and applications of polyacrylamide. Rev Roum Chim 63:143

Caravaca F, Lozano Z, Rodriguez-Caballero G, Roldan A (2017) Spatial shifts in soil microbial and degradation of pasture cover caused by prolonged exposure to cement dust. Land Degrad Dev. https://doi.org/10.1002/ldr.2564

Chang I, Prasidhi AK, Im J, Shin HD, Cho GC (2015) Soil treatment using microbial biopolymers for anti-desertification purposes. Geoerma. https://doi.org/10.1016/j.geoderma.2015.04.006

Chen H, Wang Q (2006) The behaviour of organic matter in the process of soft soil stabilization using cement. B Eng Geol Environ 65:445–448

El-Attar MM, Sadek DM, Salah AM (2017) Recycling of high volumes of cement kiln dust in bricks industry. J Clean Prod. https://doi.org/10.1016/j.jclepro.2016.12.082

Helming K, Rubio JL, Boardman J (2006) Soil erosion across Europe: research approaches and perspectives. Catena. https://doi.org/10.1016/j.catena.2006.03.008

Kaniraj SR, Havanagi VG (1999) Compressive strength of cement stabilized fly ash-soil mixtures. Cem Concr Res 29:673–677

Kawamura M, Kasai Y (2006) Compressive strength and density of fly-ash substituted soil-cement concrete. Environ Ecol Tech Concrete 302-303:376–383

Kumar MA, Raju GVRP (2009) Use of lime cement stabilized pavement construction. Ind J Eng Mat Sci 16:269–276

Li Y, Ling XZ, Su L, An LS, Li P, Zhao YY (2018) Tensile strength of fiber reinforced soil under freeze-thaw condition. Cold Reg Sci Technol 146:53–59

Liu J, Bai YX, Song ZZ, Wang Y, Chen ZH, Wang QY, Kanungo DP, Qian W (2018) Effects of basalt fiber on the strength properties of polymer reinforced sand. Fiber Polym. https://doi.org/10.1007/s12221-018-8507-2

Liu J, Chen ZH, Kanungo DP, Song ZZ, Bai YX, Wang Y, Li D, Qian W (2019) Topsoil reinforcement of sandy slope for prevent erosion using water-based polyurethane soil stabilizer. Eng Geol. https://doi.org/10.1016/j.enggeo.2019.03.003

Liu J, Feng Q, Wan Y, Bai YX, Wei JH, Song ZZ (2017) The effect of polymer-fiber stabilization on the unconfined compressive strength and shear strength of sand. Adv Mater Sci Eng:2370763

Mirzababaei M, Arulrajah A, Horpibulsuk S, Soltani A, Khayat N (2018) Stabilization of soft clay short fibers and poly vinyl alcohol. Geotext Geomembr. https://doi.org/10.1016/j.geotexmem.2018.05.001

Mohsin MA, Attia NF (2015) Inverse emulsion polymerization for the synthesis of high molecular weight polyacrylamide and its application as sand stabilizer. Int J Polym Sci 436583

Najim KB, Mahmod ZS, Atea AKM (2014) Experimental investigation on using cement kiln dust (CKD) as a cement replacement material in producing modified cement mortar. Constr Build Mater. https://doi.org/10.1016/j.conbuildmat.2014.01.015

Reis JML, Carneiro EP (2012) Mechanical characterization of sisal fiber reinforced polymer mortars: compressive and flexural properties. J Reinf Plast Compos 31:1662–1669

Rekha LA, Keerthana B, Ameerlal H (2016) Performance of fly ash stabilized clay reinforced with human hair fiber. Geomech Eng 10:677687

Tang CS, Wang DY, Cui YJ, Shi B, Li J (2016) Tensile strength of fiber-reinforced soil. J Mater Civ Eng:04016031

Wan CF, Fell R (2004) Investigation of rate of erosion of soils in embankment dams. J Geotech Geoenviron. https://doi.org/10.1061/(ASCE)1090-0241(2004)130:4(373)

Wang YL, Zhang G, Wang AX (2018) Block reinforcement behavior and mechanism of soil slopes. Acta Geotech 13:1155–1170

Xiao M, Shwiyhat N (2012) Experimental investigation of the effects of suffusion on physical and geomechanic characteristics of sandy soils. Geotech Test J. https://doi.org/10.1520/GTJ104594

Ye B, Cheng ZR, Liu C, Zhang YD, Lu P (2017) Liquefaction resistance of sand reinforced with randomly distributed polypropylene fibres. Geosynth Int. https://doi.org/10.1680/jgein.17.00029

Zang YX, Gong W, Liu BL, Chen HL (2019) Effects of different segments in polyurethane on the performance of sand stabilization. J Appl Polym Sci 47267